B. Béri
Department of Applied Mechanics,
Budapest University of Technology
and Economics,
Budapest 1521, Hungary
e-mail: beri.bence@gmail.com

G. Stépán
Department of Applied Mechanics,
Budapest University of Technology
and Economics,
Budapest 1521, Hungary
e-mail: stepan@mm.bme.hu

S. J. Hogan
Department of Engineering Mathematics,
University of Bristol,
Bristol BS8 1UB, UK
e-mail: s.j.hogan@bristol.ac.uk

Effect of Potential Energy Variation on the Natural Frequency of an Euler–Bernoulli Cantilever Beam Under Lateral Force and Compression

A cantilever beam is subjected to both lateral force and compression under gravity. By taking into account the potential energy variation of the system, we develop a theoretical result that greatly simplifies the bending vibration frequency calculation in agreement with the experiments. [DOI: 10.1115/1.4036094]

1 Motivation

Classical beam theory neglects the displacement in the direction of the beam axis when a cantilever beam is subject to a lateral force at the free end. This displacement modifies the potential energy of the system. While the natural frequency calculation uses linear theory and small displacements, the second-order nonlinear deflection of the beam has a relevant effect, in this case, on the linear vibrations. This makes the standard approximations based on the linear theory of strength of materials unsatisfactory.

As an example, consider an apple attached to the branch by means of the stem [1]. The mass of the stem is negligible compared to that of the apple. The stem is elastic and the natural frequency of the apple depends on the lateral deformation of the stem, which is affected by the tension caused by the weight of the apple. During the linear vibration of the apple, the change of the potential energy related to the vertical position of its center of gravity due to the deformation of the stem should be taken into account: the vertical displacement is a second degree function of the lateral displacement, similarly to the planar pendulum.

There is another phenomenon that might be taken into account in natural frequency calculations, namely that the tensile force caused by the weight of the apple at the end of the stem results in the variation of the lateral spring stiffness of the stem. Further clarification is needed to discuss the two kinds of potential energy variations and their effects on the natural frequency.

The objective of this study is to provide a closed-form analytical estimation of the basic natural frequency of a vertical cantilever beam with a heavy block attached to its free end (see the arrangement in Fig. 1). The beam is considered to be prismatic, homogeneous, linearly elastic, and inextensible. It is either in compression or in tension depending on whether it stands upward or downward, respectively.

To support the calculation of the potential energy, we are going to construct a simple analytic formula that describes the connection of the lateral and longitudinal displacements of an elastic beam. There have been many related results in the literature: Borboni and De Santis [2] and Lee [3] have investigated a cantilever beam under combined loads with Ludwick type material and provided a numerical algorithm to solve the problem. González and LLorca [4] examined a similar problem in the case of linearly

elastic curved beams and derived an implicit analytical expression that still requires the application of some numerical methods. Solano-Carrillo [5] has found a relationship between the geometrical and material nonlinearities concerning a beam under combined loading and suggested a semi-exact solution.

The model used by Beléndez et al. [6] is the one described in the introduction above. The mathematical model of their work is obtained from the Euler–Bernoulli curvature and bending moment connection and considered large and small deflections. They investigated only the longitudinal displacement of the beam and did not take into account its connection with the lateral displacement. Their results were achieved by incorporating some numerical methods and these were compared with experimental ones.

2 Experiment

In order to identify precisely the effect of the longitudinal displacement of a cantilever beam on the natural frequency of the bending vibration, an experimental setup was built (see Fig. 1). In the case of three different beam lengths, the natural frequencies
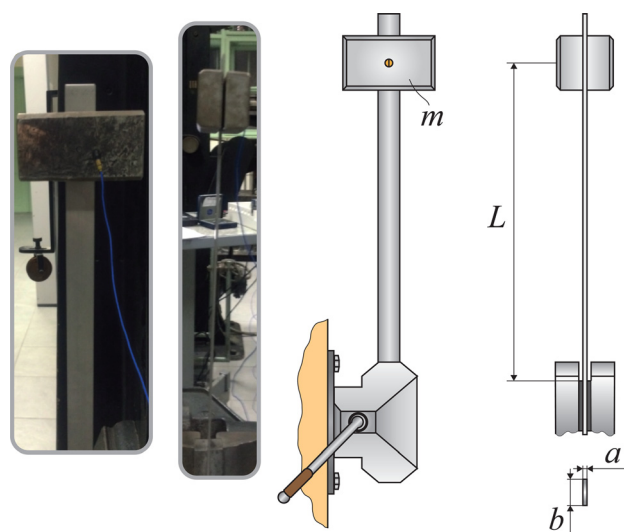
Fig. 1 The experimental equipment that consists of a rectangular cross rod with length L and a heavy block with mass $m = 0.978$ kg

Table 1 Measured natural frequencies. Three cases of load type are given.

Beam length (m)	Compression (Hz)	Neutral (Hz)	Tension (Hz)
0.30	2.513	2.720	2.910
0.40	1.525	1.750	1.950
0.50	0.975	1.231	1.460

were measured while the beam was in the vertical position under either compression or tension (depending on whether it stood upward or downward).

The horizontal position defined the neutral case, that is, the beam is not affected by the heavy block. The results of the experiment are summarized in Table 1. The average 15% difference of the frequencies depending on the longitudinal load type compared to the neutral case gives the motivation of this study: in an industrial project, simple closed-form expressions are needed for the calculation of the natural frequency of a cantilever beam with a heavy mass attached to its end, which takes into account whether the beam is vertical or horizontal. The material and geometrical data of the measured system can be found in Table 2.

3 Theory

According to the results of Beléndez et al. [6], we are able to specify

$$\xi = \kappa \eta^2 \tag{1}$$

that describes the connection of the longitudinal displacement ξ and the lateral displacement η of a cantilever beam subjected to a lateral force F at its end (see Fig. 3).

To approximate the value of κ, let us assume that the end of a cantilever beam moves on the arc of a circle (see Fig. 2). Then, by Pythagoras

$$L^2 = (L - \xi)^2 + \eta^2 \quad \Rightarrow \quad \xi^2 - 2L\xi + \eta^2 = 0$$

so ξ is given by
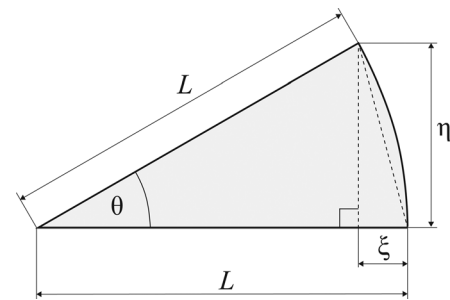
$$\xi = \frac{1}{2}\frac{\eta^2}{L} + \mathcal{O}(\eta^4) \tag{2}$$

The assumption provides the approximation of $\kappa = 1/(2L)$ where L denotes the length of the beam.

4 Modeling and Analysis

The liner mathematical model of the Euler–Bernoulli elastic beam [7] assumes the form

$$y''(x) = -\frac{M(x)}{IE} \tag{3}$$

Fig. 2 Approximation of the displacement of the end of the cantilever beam

where y describes the planar lateral deformation of the beam as a function of the coordinate x as shown in Fig. 3, while M denotes the bending moment. The cantilever prismatic beam has length L, it is inextensible, and its bending stiffness is IE with modulus of elasticity E and area moment of inertia I.

The beam is subjected to a lateral force F and compression P at its free end. Since the bending moment function can be expressed as

$$M(x) = P(y(x) - y(L)) + F(x - L)$$
$$= P\eta + F\xi \tag{4}$$

the governing equation assumes the form

$$y''''(x) + \alpha^2 y''(x) = 0, \quad \alpha^2 = \frac{P}{IE} \tag{5}$$

with boundary conditions

$$y(0) = 0, \quad y'(0) = 0, \quad y''(L) = 0$$
$$IEy'''(L) = -Py'(L) - F$$

The scalar parameters A, B, C, D of the general solution

$$y(x) = A + Bx + C\cos(\alpha x) + D\sin(\alpha x) \tag{6}$$

are determined by the above boundary conditions, which leads to the specific solution

$$y(x; F) = \left(\frac{\tan(\alpha L)}{\alpha}(1 - \cos(\alpha x)) - \left(x - \frac{\sin(\alpha x)}{\alpha}\right)\right)\frac{F}{\alpha^2 IE} \tag{7}$$

where its dependence on the lateral force F is emphasized. Then, the lateral deformation of the end of the beam η is given by

$$\eta = y(L; F) \tag{8}$$

from which the lateral force is obtained in the form

Table 2 Experimental data for Figs. 1 and 9

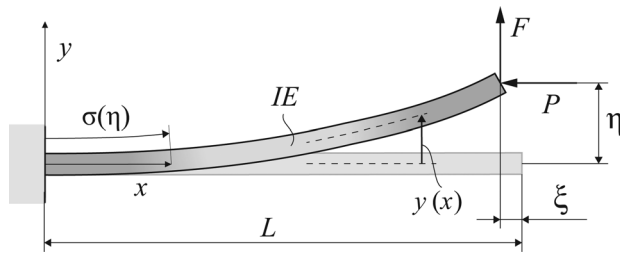| Notation	Designation	Value	Unit
ρ	Density of beam	7900	kg/m^3
E	Young's modulus of beam	200	GPa
a	Thickness of cross section	0.0020	m
b	Width of cross section	0.0203	m
L	Length of beam	0.30; 0.40; 0.50	m
m	Mass of end body	0.978	kg
m_b	Mass of beam	0.096; 0.128; 0.160	kg
J_C	Moment of inertia of end body	0.00028	kg m^2
—	Size of end body (one block)	0.01865 × 0.07915 × 0.04265	m × m × m

Fig. 3   Mechanical model of a cantilever beam

$$F(\eta) = \frac{\alpha^3 IE}{\tan(\alpha L) - \alpha L}\eta$$

The denominator of $F(\eta)$ vanishes when $\tan(\alpha L) = \alpha L$. The first root, $\alpha L = 0$, corresponds to rigid body motion. The second root, $\alpha L = \pi/0.7$, corresponds to the Euler critical load for the problem of fixed-rolling beam under compression depicted in Fig. 4.

The substitution of $F(\eta)$ into the solution Eq. (7) leads to the lateral deformation function $y(x; F(\eta))$, and the arc length of the deformed beam $\sigma(\eta)$ can also be calculated as a function of η

$$\sigma(\eta) = \int_0^{L-\kappa\eta^2} \sqrt{1 + \left(\frac{\partial y(x; F(\eta))}{\partial x}\right)^2}\, dx \qquad (9)$$

Its dependence on the end point lateral deformation η is complicated due to the presence of η in the upper limit of the definite integral, where κ is the unknown parameter we need to determine in Eq. (1). By means of the Leibniz's theorem for differentiation of an integral [8], the power series of σ can be expressed with respect to η in the form

$$\sigma(\eta) = \sigma(0) + \sigma'(0)\eta + \frac{1}{2!}\sigma''(0)\eta^2 + \cdots$$

where it is obvious that $\sigma(0) = L$ and $\sigma'(0) = 0$ because when $\eta = 0$, that is, the displacement of the end of the beam is zero, then gradient of the arc length is zero, too. The second derivative of σ at zero can be considered as

$$\sigma''(0) = -2\kappa + \int_0^{L-\kappa\eta^2} \frac{\partial^2}{\partial\eta^2}\left(\sqrt{1 + \left(\frac{\partial y(x; F(\eta))}{\partial x}\right)^2}\right) dx\bigg|_{\eta=0}$$

It assumes the form

$$\sigma(\eta) = L + (-2\kappa + \chi)\frac{\eta^2}{2!} + \cdots \qquad (10)$$

where

$$\chi = \frac{\left(1 + \frac{1}{2}\cos(2\alpha L)\right)\alpha^2 L - \frac{3}{4}\alpha\sin(2\alpha L)}{(\alpha L\cos(\alpha L) - \sin(\alpha L))^2}$$

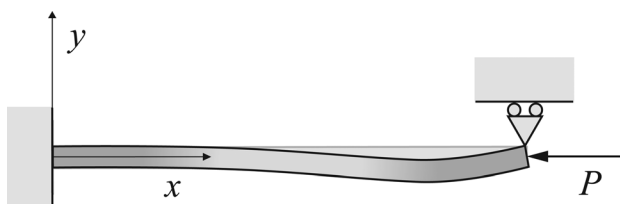Because the beam is considered to be inextensible, the arc length is L for all values of η, so

Fig. 4   Fixed-rolling beam under compression

$$\sigma(\eta) \equiv L \iff \kappa = \chi/2$$

is obtained from Eq. (10), and

$$\kappa = \frac{2(2 + \cos(2\alpha L))\alpha^2 L - 3\alpha\sin(2\alpha L)}{8(\alpha L\cos(\alpha L) - \sin(\alpha L))^2} \qquad (11)$$

The parameter α depends on the compression P (see Eq. (5)), and the parameter κ can be developed as a dimensionless power series of P

$$\kappa L = \frac{3}{5} + \frac{1}{175}\left(\frac{L^2 P}{IE}\right) + \frac{1}{2625}\left(\frac{L^2 P}{IE}\right)^2 + \cdots \qquad (12)$$

where κ is normalized by the length of the beam L and $L^2 P/IE$ represents the relative importance of compression to the proportional part of Euler buckling load. The coefficient κ in Eq. (1) agrees with the numerical evaluation of the formula in Ref. [6], which gives the four-digit-accurate value of 0.5988 that is a good approximation of 3/5 at zero compression. There is 20% difference between this exact solution and the approximation of 1/2 of the triangle in terms of the cantilever beam (see Eq. (2)). The nonzero compression obviously increases the magnitude of the longitudinal displacement of the rod as it is also expressed by formula Eq. (12) analytically.

Under tension, the only change in Eq. (12) is the sign of P. The nonzero tension decreases the magnitude of the longitudinal displacement of the beam as we can see in Fig. 5(a). Equation (11) can be transformed to a dimensionless expression by means of $(\alpha L)^2 = PL^2/(IE)$. When $L^2 P/IE \to -\infty$ by using L'Hospital's rule, $\kappa L = 1/2$ as in Fig. 2. This means that bending is negligible compared to tension and so the beam behaves according to the circular-arc approximation in Fig. 2.

Note that the expressions of κ are not uniformly valid when $F = 0$ due to the assumption of the inextensible nature of the beam.

4.1 Stiffness of Compressed Beam.
With the help of Eqs. (7) and (8), an equivalent lateral stiffness

$$k = \frac{F}{\eta} \qquad (13)$$

can be calculated with respect to the free end of the beam where the lateral force F is applied. After simplification, we obtain

$$k = \frac{\alpha^3 IE}{\tan(\alpha L) - \alpha L} \qquad (14)$$

which can be approximated by the dimensionless power series

$$\frac{L^3 k}{IE} = 3 - \frac{6}{5}\left(\frac{L^2 P}{IE}\right) - \frac{1}{175}\left(\frac{L^2 P}{IE}\right)^2 - \cdots \qquad (15)$$

Clearly, the compression decreases the lateral stiffness of the beam (see Fig. 5(b)) where the curve crosses the horizontal axis, there is the first normalized Euler buckling load. In contrast, tension increases the stiffness.

If there is a large lumped mass at the free end of the vertical beam (see Fig. 1), the bending vibration frequency can be calculated either by means of this reduced lateral stiffness or by means of the variation of the potential energy of the lumped mass in the gravitational space due to the deformation ξ. In what follows, the nonlinear equivalence of the two approaches is proven.

4.2 Proving With Energy Method.
In the case of elastic bodies, the external forces are also going to perform work when
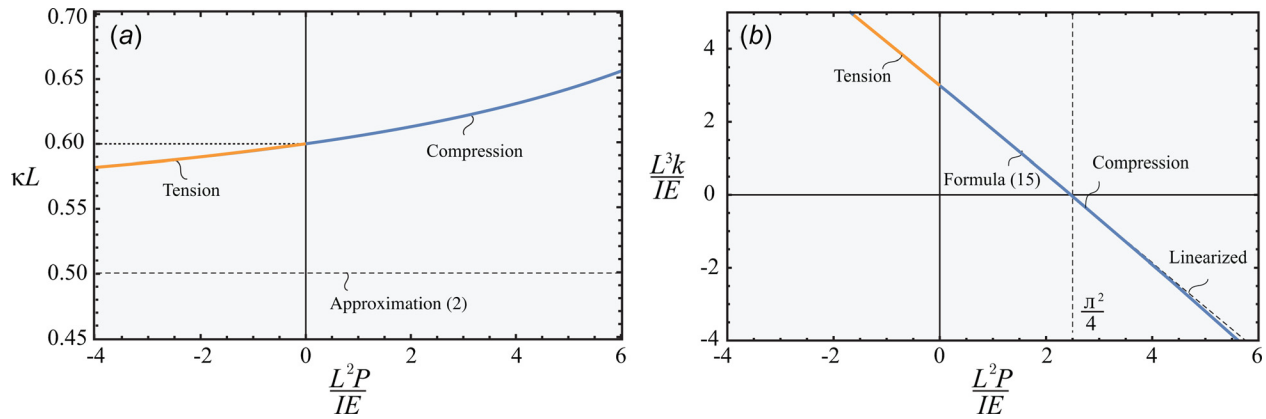
Fig. 5 (*a*) Dimensionless relationship between κL and the relative importance of compression/tension given by Eq. (12). (*b*) Dimensionless relationship between relative importance of spring stiffness and the relative importance of compression/tension given by Eq. (15).

the points of application of these forces are shifted by the effect of another applied force. The loads above are progressively increased from their zero values to their supreme values. Let us consider the point of application of $\mathbf{F}_i$ that moves with unit vector $\mathbf{e}_i$. If the relationship is linear between the load and the displacement, then the performed work is

$$W_i = \frac{1}{2}\mathbf{F}_i\mathbf{e}_i$$

If d_i is a displacement component of $\mathbf{e}_i$ in the force direction, it yields

$$W_i = \frac{1}{2}F_i d_i$$

According to the Betti's theorem, if a balanced elastic body with arbitrary shape loaded sequentially by two different equilibrium force systems included forces and couples, then they are signed by index 1 and index 2, respectively.

First of all, the elastic body is loaded by the force system of index 1 that is going to perform work W_{11}. After that, we have to apply the force system of index 2, which also performs work W_{22}; however, the second force system gives rise to further strain; hence, we need to take into account the work of the first force system, too, that provides another work signed by W_{12}. At the end of the loading period, the total work is

$$W = W_{11} + W_{22} + W_{12} \tag{16}$$

where the proper work of the force systems is denoted by W_{11} and W_{22} as well as $W_{12} = W_{21}$ are extraneous works. Note that in this case, the connection between the effects of forces and displacements is linear.

The aim is to prove that the strain energy of the described system defined by the stiffness of the beam corresponds with the work of external forces using the end displacements of the beam, that is, $U = W$. The strain energy can be written as

$$U = \frac{1}{2IE}\int_0^L M^2(x)\,\mathrm{d}x \tag{17}$$

where the function of the bending moment is defined by Eq. (4). After the substitution of Eqs. (4) and (7) into Eq. (17), we obtain

$$U = \frac{F^2}{4\alpha^3 IE}\left(\frac{\alpha L}{\cos^2(\alpha L)} - \tan(\alpha L)\right) \tag{18}$$

that can also be expressed by its power series with respect to compression P

$$U = \frac{F^2 L^3}{IE}\left(\frac{1}{6} + \frac{2}{15}\left(\frac{L^2 P}{IE}\right) + \frac{17}{210}\left(\frac{L^2 P}{IE}\right)^2 + \cdots\right) \tag{19}$$
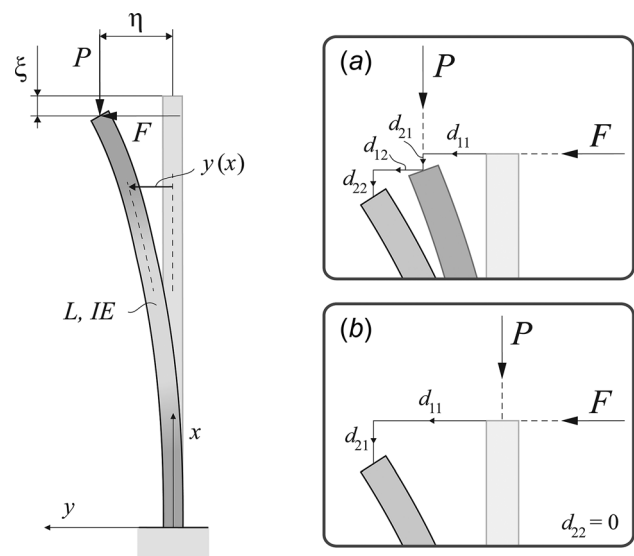
The investigation of the work done by external forces is more complicated. In order to introduce some simplifications, let us consider Eqs. (1) and (8) where the compression P is emphasized

$$\xi(P) = \frac{F^2(2\alpha L(2 + \cos(2\alpha L)) - 3\sin(2\alpha L))}{8(IE)^2 \alpha^5 \cos^2(\alpha L)}$$
$$\eta(P) = \frac{F(\tan(\alpha L) - \alpha L)}{IE\alpha^3} \tag{20}$$

The forms of their power series yield

$$\xi(P) = \frac{F^2 L^5}{(IE)^2}\left(\frac{1}{15} + \frac{17}{315}\left(\frac{L^2 P}{IE}\right) + \frac{31}{945}\left(\frac{L^2 P}{IE}\right)^2 + \cdots\right) \tag{21}$$

Fig. 6 Displacement analysis. The displacements of d_{11} and d_{21} are affected by the lateral force F. The d_{12} and d_{22} are due to compression P.

and

$$\eta(P) = \frac{FL^3}{IE}\left(\frac{1}{3} + \frac{2}{15}\left(\frac{L^2P}{IE}\right) + \frac{17}{315}\left(\frac{L^2P}{IE}\right)^2 + \cdots\right) \qquad (22)$$

respectively.

The first case can be seen in Fig. 6(a) where we assume that the lateral force F is applied first, that is, it is the first force and compression P is the second one. Note that the extraneous works are not equal; hence, the supposition of the Betti's theorem that all forces are linear in the displacements does not hold. Henceforth, Fig. 7(a) and Eq. (16) will be referred to frequently.

The lateral force is applied first that gives rise to two displacements in different directions but only one of them provides work because we do not even have compression. Since the relationship between F and d_{11} is linear

$$\begin{aligned}W_{11} &= \frac{1}{2}Fd_{11}\\&= \frac{1}{2}F\eta(0)\\&= \frac{F^2L^3}{6IE}\end{aligned} \qquad (23)$$

that means the area of a triangle in Fig. 7(a). The situation is more complicated in the case of W_{22} because the connection here is nonlinear, thus

$$\begin{aligned}W_{22} &= \int_0^L P\mathrm{d}x = P(\xi(P) - \xi(0)) - \int_0^P \xi(P) - \xi(0)\mathrm{d}P\\&= \frac{F^2\left(\alpha L\left(12 + 2\alpha^2L^2 + \dfrac{3}{\cos^2(\alpha L)}\right) - 15\tan(\alpha L)\right)}{12IE\alpha^3}\end{aligned} \qquad (24)$$

that is given by its power series

$$W_{22} = \frac{F^2L^3}{IE}\left(\frac{17}{630}\left(\frac{L^2P}{IE}\right)^2 + \frac{62}{2835}\left(\frac{L^2P}{IE}\right)^3 + \cdots\right) \qquad (25)$$

Since ξ depends only on compression P, we needed to calculate the area of W_{22} this way (see Fig. 7(a)). Finally, we examine W_{12}. The displacement is caused by compression P in the direction of the lateral force F that means a rectangular area in F–y plane; hence, the connection is also linear

$$\begin{aligned}W_{12} &= F(\eta(P) - \eta(0))\\&= -\frac{F^2\left(3\alpha L + \alpha^3L^3 - 3\tan(\alpha L)\right)}{3IE\alpha^3}\end{aligned} \qquad (26)$$
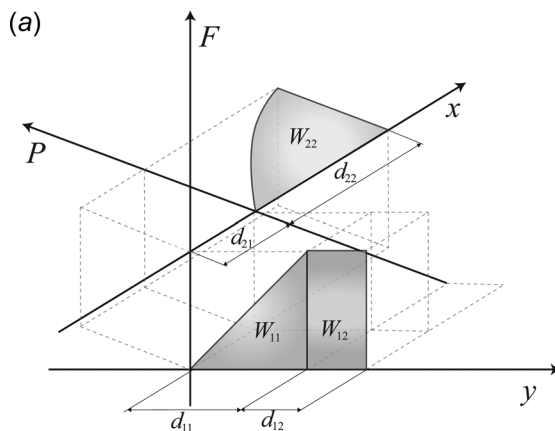
expressed by its power series

$$W_{12} = \frac{F^2L^3}{IE}\left(\frac{2}{15}\left(\frac{L^2P}{IE}\right) + \frac{17}{315}\left(\frac{L^2P}{IE}\right)^2 + \cdots\right) \qquad (27)$$

The summation of Eqs. (23), (24), and (26) provides

$$W = \frac{F^2}{4\alpha^3IE}\left(\frac{\alpha L}{\cos^2(\alpha L)} - \tan(\alpha L)\right) \qquad (28)$$

given by its power series

$$W = \frac{F^2L^3}{IE}\left(\frac{1}{6} + \frac{2}{15}\left(\frac{L^2P}{IE}\right) + \frac{17}{210}\left(\frac{L^2P}{IE}\right)^2 + \cdots\right) \qquad (29)$$

that exactly corresponds with the strain energy (see Eqs. (18) and (19)).

The second case can be seen in Fig. 6(b) where compression P is assumed to be the first force. As we consider the stiffness of the beam to be infinitely large in the beam direction, compression does not cause displacement ($d_{22} = 0$) that implies $W_{22} = 0$. When the lateral force F appears, it causes two displacements d_{11} and d_{21}. The work W_{11} is actually the area of a triangle because F was increased uniformly up to its supreme value

$$\begin{aligned}W_{11} &= \frac{1}{2}F\eta(P)\\&= \frac{F^2(\tan(\alpha L) - \alpha L)}{2IE\alpha^3}\end{aligned} \qquad (30)$$

expressed by its power series

$$W_{11} = \frac{F^2L^3}{IE}\left(\frac{1}{6} + \frac{1}{15}\left(\frac{L^2P}{IE}\right) + \frac{17}{630}\left(\frac{L^2P}{IE}\right)^2 + \cdots\right) \qquad (31)$$

The work W_{21} can be defined as a rectangular area (see Fig. 7(b)) because the value of compression was constant during the application of F

$$\begin{aligned}W_{21} &= P\xi(P)\\&= \frac{F^2(2\alpha L(2 + \cos(2\alpha L)) - 3\sin(2\alpha L))}{8IE\alpha^3\cos^2(\alpha L)}\end{aligned} \qquad (32)$$

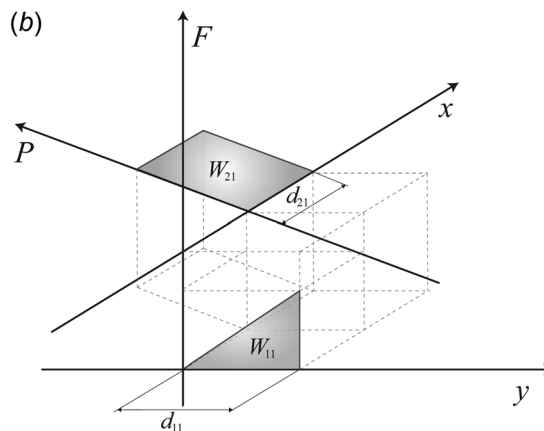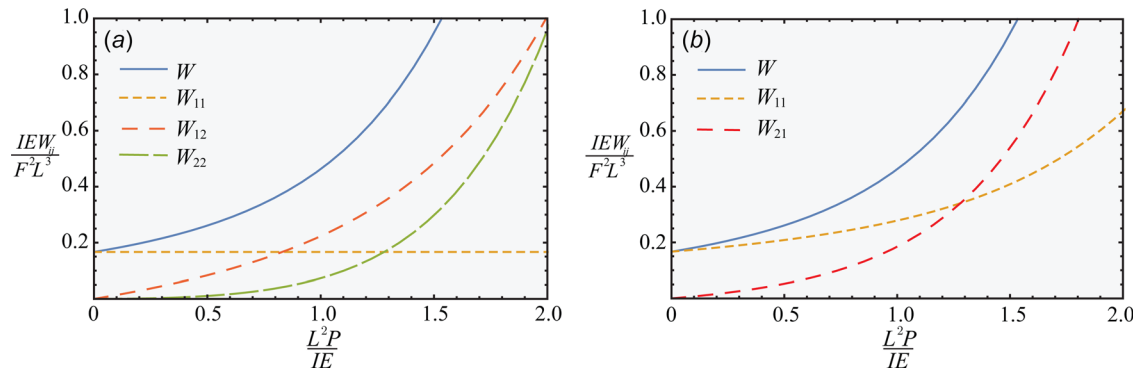given by its power series

(a)

(b)

Fig. 7   Works of external forces

Fig. 8 Dimensionless connection between the normalized works and the relative importance of compression: (*a*) case 1 and (*b*) case 2

$$W_{21} = \frac{F^2L^3}{IE}\left(\frac{1}{15}\left(\frac{L^2P}{IE}\right) + \frac{17}{315}\left(\frac{L^2P}{IE}\right)^2 + \cdots\right) \quad (33)$$

The summation of Eqs. (30) and (32) provides the same result such as Eq. (28).

So, the effect of the displacement in the rod direction results in the same potential energy variation as the equivalent stiffness modification by loads. It can be seen in Fig. 8, too.

4.3 Investigation of the Natural Frequencies of the System.
The main purpose of the investigation was to be able to determine how the natural frequencies of the system are modified by combined loads. The dynamical model of the loaded cantilever beam that can be seen in Fig. 9 describes a simple two degrees-of-freedom system. It consists of an elastic cantilever beam of length L and mass m_b and a body of mass m attached to the free end. To proceed, we assume a concentrated mass m_c at the free end of the beam. We take $m_c = m + 0.2404m_b$, where the coefficient of m_b comes from a continuum beam whose first natural frequency is approximated by a simple spring–mass system. The end mass m_c can model either compression or tension but we examine the compressed beam in particular.

The generalized coordinates are defined by the horizontal displacement of the end mass (in the direction x) and the angle φ of rotation of the beam end. In order to investigate the motion of the system above, we need to define its kinetic energy, that is

$$T = \frac{1}{2}m_c\mathbf{v}_C^2 + \frac{1}{2}J_C\omega^2 \quad (34)$$

where J_C is the moment of inertia of the end body and ω is the angular velocity that corresponds with $\dot\varphi$. The velocity of the center of gravity of the end body is denoted by $\mathbf{v}_C$ that can be described as

$$\mathbf{v}_C = \begin{pmatrix} \dot{x} \\ -\dot{h} \end{pmatrix} \quad (35)$$

where h is equal to κx^2 from Eq. (1). If the zero position of the potential function is defined at the center of gravity of the end body in the case of equilibrium, then the expression of the potential energy is

$$U = \frac{1}{2}\begin{pmatrix} x & \varphi \end{pmatrix}\mathbf{K}_r\begin{pmatrix} x \\ \varphi \end{pmatrix} - m_cgh \quad (36)$$

where $\mathbf{K}_r$ is the stiffness matrix of the rod that comes from the compliance matrix and there is an additional term ($-m_cgh$) caused by the longitudinal displacement. In terms of Eqs. (34) and (36), the linear matrix coefficient differential equation assumes the form

$$\mathbf{M}\ddot{\mathbf{q}} + \mathbf{K}\mathbf{q} = 0 \quad (37)$$

where the mass matrix is denoted by $\mathbf{M}$, the stiffness matrix is defined as

$$\mathbf{K} = \left.\frac{\partial^2 U}{\partial q_i \partial q_j}\right|_{\mathbf{q}=0}$$

and $\mathbf{q}$ means the generalized coordinates vector. The difference between our theory and the general theory is manifested by the first element (K_{11}) of the stiffness matrix

$$\mathbf{K} = \begin{pmatrix} \dfrac{12IE}{L^3}\boxed{-2m_cg\kappa} & -\dfrac{6IE}{L^2} \\ -\dfrac{6IE}{L^2} & \dfrac{4IE}{L} \end{pmatrix} \quad (38)$$

where the boxed expression decreases the magnitude of K_{11} and m_{cg} defines the compressive force P.

When P reaches its critical value, then

$$\det \mathbf{K} = 0 \quad \Rightarrow \quad \frac{3IE}{L^3} - 2P_{cr}\kappa = 0 \quad (39)$$

To approximate the critical value of compression, let us use the first approximation of κ (see the first term in Eq. (12)). Then the solution of Eq. (39) leads to $P_{cr} = 10IE/(2L)^2$ that means 1.3%
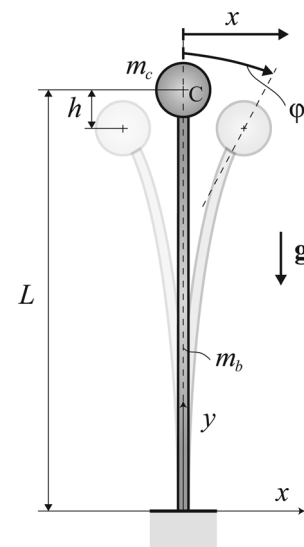
Fig. 9 Dynamical model of the two degrees-of-freedom compressed cantilever beam

Table 3 Analytical results for the first natural frequency of the system. The error columns mean the difference from the measured results that can be seen in Table 1.

Beam length (m)	Compression		Neutral		Tension	
	Results (Hz)	Error (%)	Results (Hz)	Error (%)	Results (Hz)	Error (%)
0.30	2.563	1.99	2.749	1.07	2.923	0.45
0.40	1.559	2.23	1.782	1.83	1.978	1.44
0.50	1.008	3.27	1.271	3.25	1.486	1.78

difference compared to the Euler critical buckling load $\pi^2 IE/(2L)^2$. The error decreases as the approximation of κ is improved, although it will not reach the Euler critical value even if the exact formula Eq. (11) of κ is used (see also Fig. 5(b)). The Euler critical value is obtained exactly if the additional tiny height variation h is calculated also as a function of the angle φ caused by a torque at the free end of the bar.

Since the model does not include damping and nonconservative forces, $\mathcal{D} = 0$, $\mathbf{Q} = 0$. The natural frequencies of the system can be calculated by means of frequency equation, that is

$$\det(-\omega_n^2 \mathbf{M} + \mathbf{K}) = 0 \tag{40}$$

The expanded form of Eq. (40) is a biquadratic equation

$$\omega_n^4 - \left(\frac{4IE}{J_C L} + \frac{12 J_C IE}{m_c L^3} - 2g\kappa\right)\omega_n^2$$
$$+ \left(\frac{12(IE)^2}{m_c J_C L^4} - \frac{8 IE g\kappa}{J_C L}\right) = 0 \tag{41}$$

that gives two positive roots where $\omega_{n1} < \omega_{n2}$. We deal with the first one because the measurement provided only the first natural frequency of the experimental equipment.

5 Results

While Eq. (41) provides only results concerning compression, the end mass is able to behave as tension where the natural frequencies are also easily calculated. Eventually, if the acceleration of gravity assumed to be zero, then we obtain the neutral case where the experimental equipment is held horizontally. The results of the compressed, tensed, and neutral beam are summarized in Table 3 by different beam lengths.

First of all, we can realize that the natural frequencies are lower in compression compared to the neutral case because it decreases the stiffness of the cantilever beam. On the other hand, tension increases the stiffness that causes higher natural frequencies. The natural frequencies also depend on the length of the beam.

The error columns of Table 3 mean the difference between the analytical and measured results (see Table 1). It can be seen that the largest relative failure is not greater than 4%. These minor discrepancies might be caused by the asymmetric disposition of the experimental equipment depending on the length of the beam, too.

6 Conclusion

A simple cantilever beam subjected to lateral force F and compression P at the free end was investigated. The paper brings up a classical topic of beam theory that assumes the displacement ξ in the beam direction might be neglected because that is a second-order function $\xi = \kappa\eta^2$ of the lateral displacement η. In terms of vibration theory, the longitudinal lifting of the end point of the beam is able to vary the potential function of the system that acts upon the natural frequencies. The investigated formula is given by its power series

$$\kappa L = \frac{3}{5} + \frac{1}{175}\left(\frac{L^2 P}{IE}\right) + \frac{1}{2625}\left(\frac{L^2 P}{IE}\right)^2 + \cdots$$

that makes up connection between the longitudinal and lateral displacements of the end of the beam in the case of compressive force P.

The question was whether the modification of the potential energy corresponds with the stiffness variation of the system under the combined loads above or not. By means of the Betti's theorem, it can be proved that the work of external loads using the longitudinal displacement equals with the strain function of the system considered only by bending.

The analytical results correspond to the measurement results where the errors might be explained by the asymmetric disposition of the device. Graff [9] has also examined the dynamics of beams and elaborated on the flexural waves in thin rods under different types of loads. He dealt with the effects of prestress in the case of a pin-ended column investigating continuum beam without end mass. The development of his models might provide another way to understand our results.

The importance of our theory is manifested by the natural frequency calculations of the blades of wind turbines and long boring tools [10–14] where large longitudinal forces might appear. There are many related theoretical, numerical results and topics in the literature: Bayly et al. [15] investigated the low frequency vibration in drilling to find agreement with drilling tests in the presence of large longitudinal cutting forces. Roukema and Altintas [16] and Heisig and Neubert [17] also considered lateral vibration of drilling tools. Park et al. [18] examined the linear vibration of blades of a wind turbine to see how to avoid structural resonance due to significant axial forces caused by rotation.

References

[1] Cooke, J., and Rand, R., 1969, "Vibratory Fruit Harvesting: A Linear Theory of Fruit-Stem Dynamics," J. Agric. Eng. Res., **14**(3), pp. 195–200.
[2] Borboni, A., and De Santis, D., 2014, "Large Deflection of a Non-Linear, Elastic, Asymmetric Ludwick Cantilever Beam Subjected to Horizontal Force, Vertical Force and Bending Torque at the Free End," Meccanica, **49**(6), pp. 1327–1336.
[3] Lee, K., 2002, "Large Deflections of Cantilever Beams of Non-Linear Elastic Material Under a Combined Loading," Int. J. Non-Linear Mech., **37**(3), pp. 439–443.
[4] González, C., and LLorca, J., 2005, "Stiffness of a Curved Beam Subjected to Axial Load and Large Displacements," Int. J. Solids Struct., **42**(5–6), pp. 1537–1545.
[5] Solano-Carrillo, E., 2009, "Semi-Exact Solutions for Large Deflections of Cantilever Beams of Non-Linear Elastic Behaviour," Int. J. Non-Linear Mech., **44**(2), pp. 253–256.
[6] Beléndez, T., Neipp, C., and Beléndez, C., 2002, "Large and Small Deflections of a Cantilever Beam," Eur. J. Phys., **23**(3), pp. 371–379.
[7] Bazant, Z., and Cedolin, L., 2010, Stability of Structures, World Scientific Publishing Co. Pte. Ltd., Singapore.
[8] Adamowitz, M., and Stegun, I., 1972, Handbook of Mathematical Functions With Formulas, Graphs and Mathematical Tables, Dover Publications, New York.
[9] Graff, K., 1975, Wave Motion in Elastic Solids, Dover Publications, New York.

[10] Jureczko, M., Pawlak, M., and Mezyk, A., 2005, "Optimisation of Wind Turbine Blades," J. Mater. Process. Technol., **167**(2–3), pp. 463–471.

[11] Kong, C., Bang, J., and Sugiyama, Y., 2005, "Structural Investigation of Composite Wind Turbine Blade Considering Various Load Cases and Fatigue Life," Energy, **30**(11–12), pp. 2101–2114.

[12] Lee, D., Hwang, H., and Kim, J., 2003, "Design and Manufacture of a Carbon Fiber Epoxy Rotating Boring Bar," Compos. Struct., **60**(1), pp. 115–124.

[13] Ema, S., and Marui, E., 2000, "Suppression of Chatter Vibration of Boring Tools Using Impact Dampers," Int. J. Mach. Tools Manuf., **40**(8), pp. 1141–1156.

[14] Ema, S., and Marui, E., 2003, "Theoretical Analysis on Chatter Vibration in Drilling and Its Suppression," J. Mater. Process. Technol., **138**(1–3), pp. 572–578.

[15] Bayly, P., Lamar, M., and Calvert, S., 2002, "Low-Frequency Regenerative Vibration and the Formation of Lobed Holes in Drilling," ASME J. Manuf. Sci. Eng., **124**(2), pp. 275–285.

[16] Roukema, J., and Altintas, Y., 2007, "Generalized Modeling of Drilling Vibrations—Part II: Chatter Stability in Frequency Domain," Int. J. Mach. Tools Manuf., **47**(9), pp. 1474–1485.

[17] Heisig, G., and Neubert, M., 2000, "Lateral Drillstring Vibrations in Extended-Reach Wells," IADC/SPE Drilling Conference, New Orleans, LA, Feb. 23–25, SPE Paper No. SPE-59235-MS.

[18] Park, J., Park, H., Jeong, S., Lee, S., Shin, Y., and Park, J., 2010, "Linear Vibration Analysis of Rotating Wind-Turbine Blade," Curr. Appl. Phys., **10**(9), pp. S332–S334.